*Int. J. Electrochem. Sci.*, 14 **(2019)** 8686 – 8698, doi: 10.20964/2019.09.28

International Journal of
ELECTROCHEMICAL
SCIENCE
www.electrochemsci.org

# Electrochemical and Optical Behavior of Microalloyed Steel in Near-Neutral Aqueous Solution

*J. Castrellon-Uribe*[1], *A. Torres-Islas*[2,*], *S. Serna*[1] *and H. Martinez*[3]

[1] Centro de Investigación en Ingeniería y Ciencias Aplicadas, CIICAp, (IICBA),
[2] Facultad de Ciencias Químicas e Ingeniería, FCQeI. Universidad Autónoma del Estado de Morelos, P.E. Ing. Mecánica, Av. Universidad No. 1001, Col. Chamilpa, C.P. 62209 Cuernavaca, Morelos, México.
[3] Laboratorio de Espectroscopia, Instituto de Ciencias Físicas, Universidad Nacional Autónoma de México, A.P. 48-3, C.P. &2210, Cuernavaca - 62210, Morelos México.
[*]E-mail: alvaro.torres@uaem.mx

*Received:* 22 January 2019 / *Accepted:* 27 June 2019 / *Published:* 31 July 2019

A comparative study is presented using optical absorbance and potentiodynamic tests for monitoring corrosion rate. Physical degradation of X-70 microalloyed steel samples over various exposure intervals is measured by optical absorbance in solutions contaminated with corrosion oxides. A laser diode at 635 nm was used for monitoring the accumulation of corrosion oxides dissolved for 30 h in NS-4 aqueous solutions of the metallic samples. The optical power of transmittance and corrosion current ($I_{corr}$) from potentiodynamic polarization tests show good agreement, with the slopes of the two curves coinciding. This agreement indicates a continuous dissolution process, confirming that the material continues to show no formation of protective metallic oxides.

**Keywords:** X-70 steel; Electrochemical measurement; Oxide film; NS-4 solution; Optical monitoring

## 1. INTRODUCTION

Corrosion rate assessment in metals and alloys is typically to perform through measurement of weight loss, or else by electrochemical techniques [1-3]. Likewise, optical techniques have been developed for corrosion monitoring, based on the holographic interferometry [4]. However, the main limitation of these techniques arises when measurements have to be taken *in situ*, under dissimilar or noncontrolled conditions. Recently, optical intensity sensors have been used for the measurement of corrosion [5,6]; similarly, several recent studies have focused their research on the application of

optical sensors and other sensor systems, such as fiber Bragg gratings, multiple-beam interferometry, and radiofrequency [7-18]. The continued investigation of new measurement alternatives is necessary in order to keep the optical- corrosion techniques field moving forward.

As a key application of corrosion research, pipeline stress corrosion cracking (SCC) is extremely important in guaranteeing pipeline safety. In the present research, the authors are concerned primarily with monitoring of the environment–metal surface interaction that promotes corrosion and SCC. Parkins [19-21] has proposed some mechanisms for high-pH SCC, whereas low-pH (near-neutral) SCC is less understood. Several authors have published their studies on hydrogen evolution and its implications for pipeline SCC [22-25], but some controversy remains concerning hydrogen evolution. However, we know that carbonate or bicarbonate species are always present in the corroding media, either in a high pH range or a low (near-neutral) pH range.

This study focuses on continuing investigations previously carried out by Castrellon-Uribe et al. [5, 27]. Here, we show the experimental results of optical and electrochemical monitoring of corrosion rate in X-70 grade microalloyed steel immersed in a NS-4 aqueous solution at room temperature for 30 h. This aqueous solution is commonly used to simulate diluted trapped water on the pipe surface under disbonded coatings [26]. The optical technique is based on the change of optical absorbance measured in solutions contaminated with corrosion oxides. This variation is related to physical degradation of the metallic samples analyzed after various exposure intervals. Likewise, corrosion rate results obtained using conventional electrochemical techniques (electrochemical noise and potentiodynamic polarization) are reported, and a brief comparative analysis connecting the two techniques is presented.

## 2. EXPERIMENTAL PROCEDURE

To monitor corrosion rate in this study, we used X-70 grade microalloyed steel immersed in NS-4 aqueous solution. X-70 microalloy is a steel alloy regularly used in the construction of pipelines for hydrocarbon transportation. This solution simulates general conditions for the vast majority of pipeline external environments, i.e., soil in the presence of water. The chemical compositions of the solution and steel, respectively, are detailed in Tables 1 and 2. The solution was prepared using distilled water and analytical grade reagents.

**Table 1.** NS4 solution composition in g/l.

| KCl | $NaHCO_3$ | $CaCl_2 \cdot 2H_2O$ | $MgSO_4 \cdot 7H_2O$ |
|---|---|---|---|
| 0.122 | 0.483 | 0.181 | 0.131 |

**Table 2.** X-70 steel chemical composition in wt %.

| C | Mn | Si | P | S | Al | Nb | Cu | Cr | Ni | Mo | Ti | Fe |
|---|---|---|---|---|---|---|---|---|---|---|---|---|
| 0.037 | 1.48 | 0.1 | 0.01 | 0.004 | 0.12 | 0.097 | 0.28 | 0.3 | 0.15 | 0.036 | 0.011 | Bal |

*2.1. Preparation of test samples and development of electrochemical tests*

Polarization curves were obtained from potentiodynamic polarization tests in NS-4 solution at room temperature. The test samples were prepared by cutting parallelepipeds (rectangular) of 0.5 cm length and 0.05 cm thickness. Subsequently, a nichrome wire was welded to one face of the sample to serve as an electrical conductor. The wire was shielded by a glass tube to prevent contact with the solution, and the sample was then encapsulated in polyacrylic resin, leaving one face of the sample exposed. The exposed surface of the sample was polished using sandpaper up to grade 600. Polarization tests were performed on the basis of ASTM G5-94. Prior to electrochemical tests, a cyanoacrylate-based adhesive was applied on the sides of the metal in contact with the resin to avoid crevice corrosion.

Potentiodynamic tests were carried out using a calibrated potentiostat/galvanostat (ACM Instruments) controlled by a computer. The potentiodynamic scan rate for corrosion monitoring was 1 mV/s, within a potential range between −100 and +900 $mV_{ECS.}$

The electrochemical cell arrangement comprised a 50-mL glass with the test solution, a stirrer, and three electrodes, the reference saturated calomel electrode (SCE), an auxiliary graphite electrode, and the working electrode (X-70 steel). The glass was placed on a grill equipped with an agitation system.

The first six tests were performed using time intervals of 2 h between tests; the seventh test was carried out after 12 h. Immediately after each electrochemical test, 1 mL of the solution was extracted to be assessed through optical test before removing the solution from the glass; this extraction was agitated to homogenize the corrosion products. To determine the corrosion current density ($I_{corr}$), Tafel extrapolation was used, taking into account the anodic branch for each polarization curve.

In addition, electrochemical noise corrosion tests were performed to determine the type of corrosion. For this test, two identical working electrodes (X-70 steel) and a reference electrode were used. The test involved registering the potential variation in time series for which a sampling frequency of 1 record/s was used, recording 1024 data points.

The main objective of the electrochemical tests was to determine the type and level of corrosion mechanism in the X-70 steel immersed in NS-4 solution. These results were then used to correlate with the results obtained through the proposed optical techniques for corrosion monitoring.

*2.2. Preparation of test samples and development of optical measurements*

An optical cell was used to perform the first experiment to monitor the spectral response of absorbance of the NS-4 aqueous solution, in particular as related to the corrosion of X-70 steel for different measurement times.

Initially, the spectral absorbance of the corrosive solution of NS-4 without contamination was measured using a tungsten halogen light source and an optical cell of parallel flat walls having dimensions of 12 × 45 × 11: width, height, depth, for a total capacity of 1.5 mL. After, 3 mL of the corrosive solution was extracted from the electrochemical cell every 2 h for 30 h, and its spectral absorbance was recorded.

The optical spectral absorbance, i.e., corrosion, was measured and analyzed at room temperature using a spectrometer (Ocean Optics) in the wavelength range of 400–1100 nm.

After that, another electrochemical experiment was performed for 30 h. A new sample of X-70 steel was used, and a new corrosive solution of NS-4 was monitored optically. The optical signal in the electrochemical cell was recorded every 2 h, and its optical power was measured at room temperature using a pigtailed laser diode. The optical power of transmittance, ΔP, was measured using an optical detector as a measure of corrosion.

Figure 1 shows the laser experimental setup employing the optical transmittance ratio technique. This setup served to monitor corrosion rates of X-70 steel immersed in NS-4 solution.

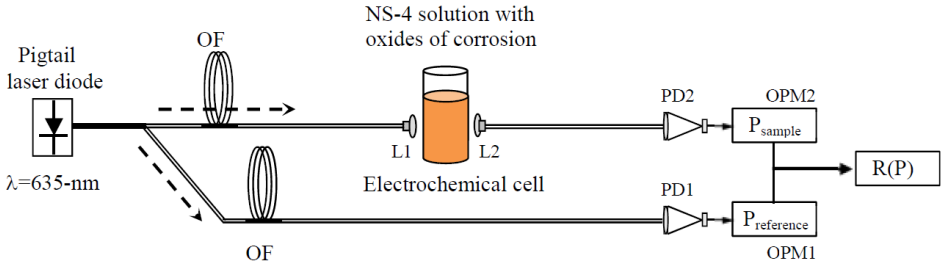


**Figure 1.** Experimental setup for optical monitoring of corrosion of X-70 samples immersed in NS-4 solution.

In this experiment, a bifurcated optical fiber 50/50 was connected to the pigtailed laser (with emission at 635 nm), which divides the optical beam into reference and transmittance signals. The signal of reference, $P_{reference}$, is measured using photodetector PD1 that is connected to optical power meter OPM1 to give 5.18 mW (after subtracting the dark signal). For the signal of transmittance, the laser beam that travels through the optical fiber is focused by biconvex lens L1 (connected at the end of the bifurcate fiber) directly on the electrochemical cell containing the corrosive solution.

Next, the optical signal of transmittance of NS-4 solution, $P_{sample}$, is confined with biconvex lens L2 toward the core of a multimode optical fiber, which transports the optical signal to photodetector PD2. The optical signal, $P_{sample}$, is measured using optical power meter OPM2 (after subtracting the dark signal). The signal of transmittance, by which corrosion is measured, is analyzed

at room temperature every 2 h for 30 h. Last, the optical signal is processed to give the power ratio of transmittance, R(P), for different concentrations of corrosion oxide dissolved in the NS-4 aqueous solution.

## 3. RESULTS AND DISCUSSION

### *3.1. X-70 steel electrochemical corrosion results*

Figure 2 displays polarization curves results for X-70 steel samples in NS-4 solution for various exposure intervals. The open-circuit potential ($E_{corr}$) showed that all of the curves were in the range of −736 to −643 $mV_{ECS}$. All of the polarization curves at their anodic regions showed asymptotic behavior, indicating purely anodic dissolution as the corrosion process. This means that, for all measured time intervals, passivation did not exist within the potential sweep range of the electrochemical tests. Previous studies have reported [6-12] that the absence of passivation is due to the retardant effect of $Cl^-$ and $SO_4^{2-}$ ions on the formation of a passive layer on the steel surface. However, the major $E_{corr}$ difference values, at 28 and 30 h, respectively, must ultimately be related to the development of corrosion products in certain areas, acting as a barrier between the solution and surface of the metal.

Variation in $I_{corr}$ was calculated using Tafel extrapolation from the polarization curves shown in Fig. 2 for the various intervals over which the polarization tests were done: 2, 4, 6, 8, 10, 24, 26, 28, and 30 h. The corresponding $I_{corr}$ and $E_{corr}$ values are shown in Table 3. As can be seen, $I_{corr}$ increases steadily from the beginning to the end of the polarization test.

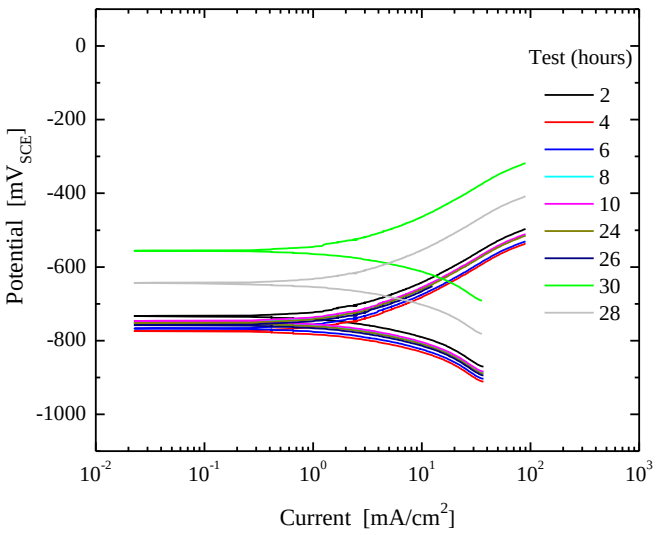


**Figure 2.** Effect of exposure time in potentiodynamic polarization test for X-70 steel samples immersed in NS-4 solution.

**Table 3.** Corrosion parameters of polarization curves for X-70 steel immersed in NS-4 solution

| Exposure time (h) | $I_{corr}$ ($mA/cm^2$) | $E_{corr}$ ($mV_{ECS}$) |
|---|---|---|
| 2 | 1.749 | −736 |
| 4 | 4.311 | −774 |
| 6 | 4.45 | −765 |
| 8 | 4.558 | −753 |
| 10 | 5.112 | −745 |
| 24 | 5.406 | −755 |
| 26 | 5.613 | −767 |
| 28 | 5.915 | −559 |
| 30 | 6.694 | −643 |

These corrosion products could decrease the rate of the corrosion process; this idea is supported by Fig. 3's results from optical microscopy analysis of certain areas of the corroded steel surface. Figure 3 shows a steel surface after the polarization test, noting areas with greater concentrations of corrosion products.

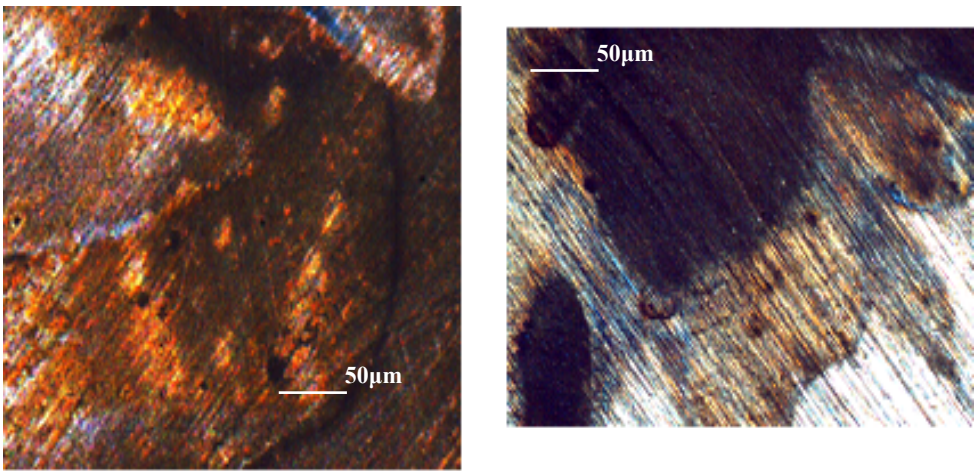


**Figure 3.** X-70 steel surface optical microscopy microphotographs after potentiodynamic polarization tests in NS-4 solution.

On the other hand, the polarization curves show the absence of passivation, which will be later evidenced by X-70 steel surface optical microscopy after electrochemical tests in NS-4 solution. The type of corrosion exhibited was uniform or generalized; this finding was confirmed by analysis of the results in potential noise time series (Fig. 4). The potential noise time series shown in Fig. 4 indicates that the potential transient has a high frequency and low intensity; these qualities are characteristic of a uniform corrosion process. The anodic potential peaks in the graph represent pits in the metal, and the cathodic potential peaks indicate steel surface repassivation.

*3.2. Optical absorbance with sensitivity to X-70 steel corrosion oxides*

In this corrosion system, various amounts of hydroxyl, carbonate, and/or bicarbonate ions can be formed. As iron ions react with carbonate ions, iron(II) carbonate ($FeCO_3$) can be formed. The resultant anodic response is the dissolution of iron to ferrous ion $Fe^{2+}$ [28]. In bicarbonate solutions, the reaction products are $Fe(OH)_2$ and/or $FeCO_3$, depending on pH and $HCO_3^-$. Therefore, dissolution reactions can be expressed as:

$$Fe + 2H_2O \rightarrow Fe(OH)_2 + 2H^+ + 2e^- \quad (1)$$

$$Fe + HCO_3^- \rightarrow FeCO_3 + H^+ + 2e^- \quad (2)$$

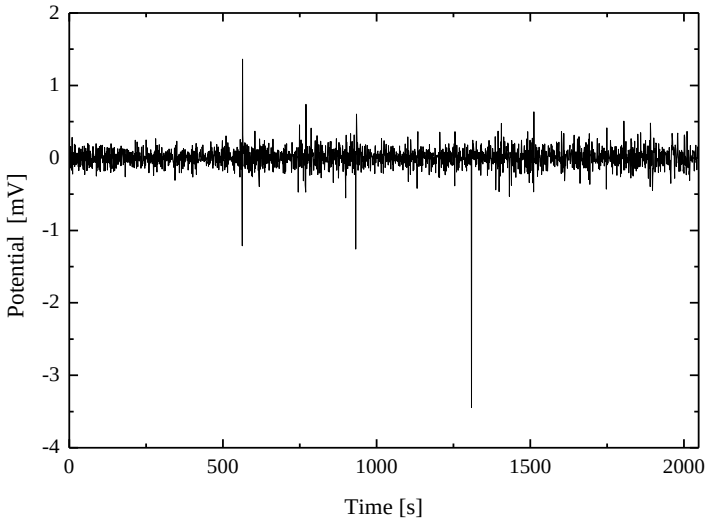


**Figure 4.** Potential noise time series for X-70 steel samples immersed in NS-4 solution.

The dissolution reaction (1), favored at high pH, is determined by the $H^+$ or ($OH^-$) concentration of the solution. Meanwhile, as $HCO_3^-$ concentrations decrease to levels between pH 8.2 and pH 9.5, no substantial effects of $HCO_3^-$ concentration on reaction (1) are expected. Yellow corrosion deposits noted are due to the presence of $FeCO_3$.

In solutions with low $HCO_3^-$concentration, it is very feasible that an oxide film of $FeCO_3$ might adhere on the steel surface. This result follows from the thermodynamic possibility of $FeCO_3$ formation in the presence of $HCO_3^-$. Therefore, dissolution and formation mechanisms simultaneous coexist when $Fe^{2+}$ diffusion through the steel-oxide film surface breaks the $FeCO_3$ equilibrium of $Fe^{2+}$ and $CO^{2-}$ ions.

Figure 5 shows the optical absorbance measured in NS-4 aqueous solution in the wavelength interval from 400 to 900 nm for several measurement intervals of the X-70 steel sample immersed in a corrosive solution, up to 30 h. The absorption of the optical radiation in the corrosive solution is

equivalent to corrosion oxide accumulation in the NS-4 solution, which is generated by the physical degradation of X-70 steel (see Fig. 3). Moreover, the corrosive solution of NS-4 after 30 h turns into orange-red owing to hoarding the accumulation of dissolved corrosion products at different concentrations. The maximum optical absorbance measured at 450 nm (blue) is ≈0.835 for 30 h of exposure. Additionally, for the wavelengths at 532 nm (green) and 635 nm (red), the maximum absorbance values are ≈0.576 and ≈0.357, respectively, for the same 30-h exposure time.

According to the above, the measured optical absorbance shows the possibility of using a laser diode with emission in 635 nm which is commercially available and at low cost; to monitor corrosion oxide accumulation in corrosive solutions which is related to the metallic corrosion of X-70 steel.

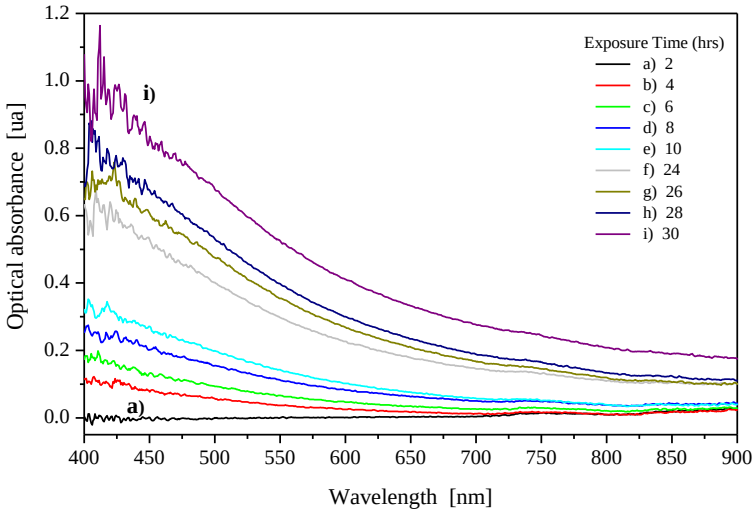


**Figure 5.** Optical absorbance measured in NS-4 aqueous solution from 400 to 900 nm of wavelength for different intervals of exposure of the X-70 steel sample in corrosive solution at 25 °C.

The optical power of transmittance of NS-4 aqueous solution contaminated with corrosion oxide products of X-70 steel was recorded by employing the optical setup shown in Fig. 1, with a laser diode (mod: HL634C) having a maximum optical output power of 10 mW at 635 nm of wavelength. In this experiment, the optical signal monitored the electrochemical cell every 2 h for 30 h. The optical power decreased from 5.14 to 4.24 mW during the first 10 h of experimentation, whereas over the next 20 h, the optical power decreased from 3.4 to 2.5 mW (Fig. 6). The change in optical power of transmittance is a function of the absorbance coefficient of the corrosive solution measured at a wavelength of 635 nm. The output optical power was recorded after subtracting the optical signal of reference, $P_{reference}$ (5.18 mW), of pure NS-4 solution without corrosion oxides. All of the optical experimentation was performed at room temperature.

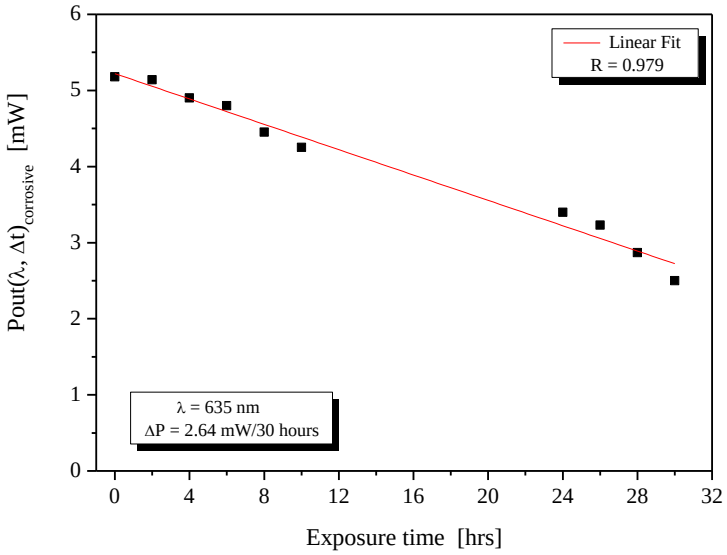


**Figure 6.** Longitudinal time series of optical power of transmittance, as measured using a laser diode at 635 nm, in NS-4 aqueous solution contaminated with corrosion oxides for 30 h. The line shows best-fit linear regression of optical power of transmittance on exposure time.

Figure 7 display the change over time of optical power of transmittance, $\Delta P$ ($\lambda$, $\rho_{oxides}$ + $\Delta t$), of NS-4 aqueous solution (measured using optical power meter) after subtracting the $P_{reference}$ (5.18 mW) of pure NS-4 aqueous solution without corrosion oxides.

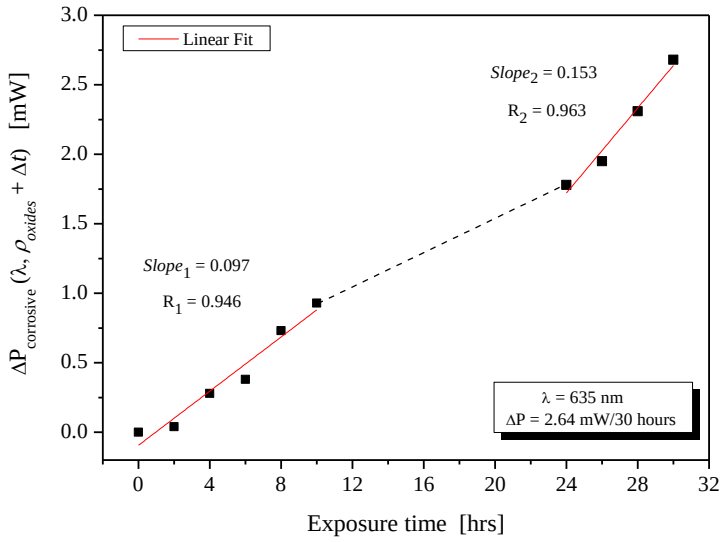


**Figure 7.** Longitudinal time series of optical power of transmittance (ΔP), as measured using a laser diode at 635 nm, in NS-4 aqueous solution contaminated with corrosion oxides for 30 h. Lines show best-fit linear regressions of optical power of transmittance on exposure time, over two disjunct subsets of the exposure interval lengths.

Optical power at a wavelength of 635 nm was recorded as a function of corrosion oxide accumulation, $\rho_{oxides}$, over an exposure interval increment, $\Delta t$, of the X-70 steel sample immersed in corrosive solution. The optical signal changed from 0.04 to 0.93 mW during the first 10 h of experimentation, whereas in the next 20 h, the optical power changed from 0.93 to 2.68 mW. The diminishing optical signal of transmittance during the immersion of the X-70 steel sample in the corrosive solution is due to the increasing concentration of corrosion oxides accumulating in the NS-4 aqueous solution as a result of X-70 steel corrosion (see Fig. 7).

Figure 7 shows that, in the first 10 h of experimentation, the slope of the curve representing the change of optical signal of transmittance (slope1 = 0.097 mW/h) was slightly smaller than that for the next few hours of the experiment. These results indicate that corrosion was slower in the first phase of the process, as showed in Fig. 7. After 10 h and until the end of the experiment, the slope of the curve representing the variation of optical signal of transmittance (slope 2 = 0.153/h) was slightly higher. These results confirm that the material still did not show the formation of protective metallic oxides; on the contrary, the material continued to experience increasing corrosive attack.

Nevertheless, the cumulative corrosion rate shows nearly linear behavior with a positive gradient, as does optical power, indicating increasing accumulation of oxides of corrosion in the solution. This finding is of critical importance, since corrosion results, not only electrochemical but also optical, are typically assumed to depend on surface complaint effects, mainly corrosion product deposition. The Ca-Mg-$CO_3$ scale frequently found on steels in environments similar to NS-4 solution has shown to greatly increase in H evolution on microalloyed steels; similarly, multilayer Fe-oxide ($Fe_3O_4$) and Fe-oxyhydroxide (α-FeOOH) formations in aqueous solutions containing $O_2$- can accelerate cathodic behavior through separation of anodic and cathodic sites. [29]

### *3.3. Optical monitoring of corrosion based on power ratio of transmittance*

The response curve of the optical technique was obtained for the change in the power ratio of transmittance, $R(P)= \Delta P_{sample}/P_{ref}$, expected to be related to the dissolution of X-70 steel samples caused by corrosive NS-4 solution over various exposure intervals. Here $\Delta P_{sample}$ is the optical power of transmittance that was measured in the corrosive solution (see Fig. 7), and $P_{ref}$ is the optical power of reference measured using the optical power meter at 5.18 mW at 635 nm.

Figure 8 shows the transmittance, R(P), and the corrosion current density, $I_{corr}$, during 30 h of experimentation. Over the 30 h of experimentation, the power ratio at 635 nm increased from $7.72 \times 10^{-3}$ to $5.144 \times 10^{-1}$; this change is related to a change in corrosion current from 17.49 to 54.06 $mA/cm^2$.

Good agreement was obtained between parameters representing optical (R(P)) and electrochemical ($I_{corr}$) measures of corrosion. This agreement is manifest in the coincident behavior of the curves of calibration of the optical and electrochemical techniques (Fig. 8).

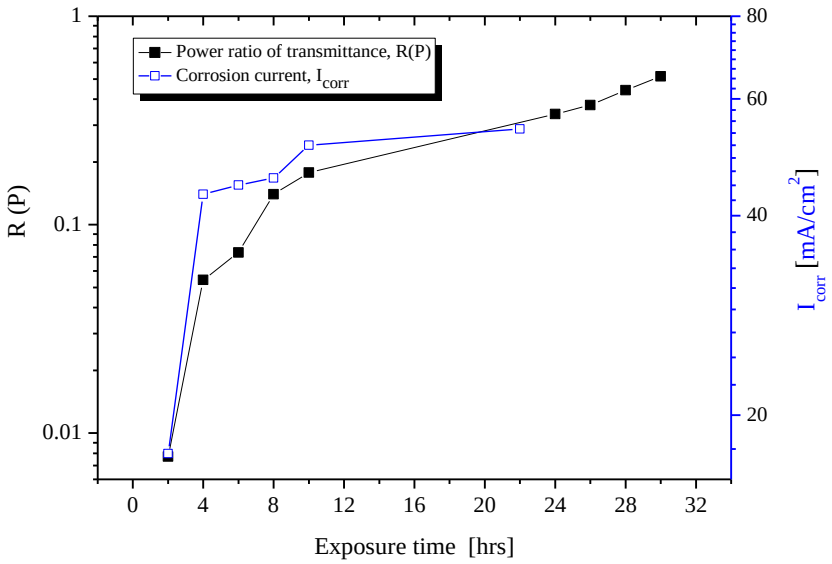


**Figure 8.** Longitudinal time series of power ratio of transmittance R(P) (optical technique) employing a laser diode at 635 nm and longitudinal time series of corrosion current ($I_{corr}$) as functions of immersion time. $I_{corr}$ data are drawn from the potentiodynamic polarization tests obtained *via* the electrochemical technique.

Of course, such agreement is not the only criterion by which to select an *in situ* corrosion monitoring method for microalloyed pipeline steel. In other optical techniques, such as optical frequency domain reflectometry (OFDR) [30], the corrosion scope along the pipe axial direction can be detected. In Liang Ren et. al.'s [30] corrosion test, several optical fiber sensors were bonded to the pipe surface, forming a sensor array, and based on the sensor array, a hoop strain nephogram was created to indicate corrosion degree and corrosion location. Their experimental method is clearly designed for *in situ* monitoring, but our $I_{corr}$ and absorbance results indicate the plausibility of an optical transmittance-based portable device for monitoring corrosion in microalloyed pipeline steel.

## 4. CONCLUSIONS

The alignment of our optical results with established electrochemical behavior confirms that the X-70 steel samples continued to show no formation of protective metal oxides after 30 h. On the contrary, the material continued to experience increasing corrosive attack. Nevertheless, increasing accumulation of corrosion oxides in the NS-4 aqueous solution were clearly related to the physical degradation of the X-70 steel samples. These findings are based on the nearly linear, positive slope of longitudinal time series of accumulated corrosion rate, as well as of change in optical power. A continuous dissolution process was indicated by the good agreement between the slopes of longitudinal time series of power ratio of transmittance and of corrosion current.

The present study demonstrates the usefulness of optical absorbance for evaluating microalloyed steel corrosion. This demonstration with steel makes optical absorbance a promising candidate technique for evaluating corrosion in other metallic materials in a variety of corrosive media.

Our results here form the basis for a forthcoming study on corrosion using optical fiber sensors in passive materials. That study explores the possibility of optical determination of corrosion product types.

## References


1. D. Piron, The electrochemistry of corrosion, National Association of Corrosion Engineers, Houston, TX., 1991.
2. P. Marcus and J. Oudar, Corrosion mechanisms in theory and practice, Marcel Dekker, Inc. USA, 1995.
3. F. Pruckner, Corrosion and protection of reinforcement in concrete measurements and interpretation, PhD thesis, University of Viena, 2001.
4. K. Habib, *Corros Sci*., 40 **(**1998)1435.
5. J. Castrellon-Uribe, C. Cuevas-Arteaga, A. Trujillo-Estrada, *Opt Laser Eng*., 46 **(**2008) 469.
6. D. Saying, L. Yanbiao, T. Qian, L. Yanan,Q. Zhigang, S. Shizde, *Corros Sci*., 48 (2006) 1746.
7. P.G. Venancio, R.A. Cottis, R. Narayanaswamy, J.C.S. Fernandes, *Sensors Actuat B-Chem.,* 182 **(**2013) 774.
8. E.C. Rios, A.M. Zimer, E.C. Pereira, L.H. Mascaro, *Electrochim Acta*, 124 **(**2014) 211.
9. E.M. Sherif, A.H. Seikh, *Int J Electrochem Sci.,* 10 (2015) 209.
10. G.U.O. Qiang, L.I.U. Jian-hua, Y.U. Mei, L.I. Song-mei. *Int J Electrochem Sci.,* 10 (2015) 701.
11. E.M. Sherif, A.A. Almajid. *Int J Electrochem Sci.,* 10 (2015) 34.
12. L. Onyeji, G. Kale. *J Mater Eng Perform.,* 26 (2017) 5741.
13. M.R. Islam, M. Bagherifaez, M.M. Ali, H.K. Chai, K.S. Lim, H. Ahmad, *IEEE T Instrum Meas.*, 64 **(**2015) 3510.
14. N. Zhang, W. Chen, X. Zheng, W. Hu, M. Gao, *IEEE Sens J*., 15 **(**2015) 3551.
15. B.R.Shrestha, Q.Hu, T. Baimpos, K. Kristiansen, J.N. Israelachvili, M. Valtiner, *J Electrochem Soc*., 162 **(**2015) C327.
16. Y. Chen, F. Tang, Y. Tang, M.J. O'Keefec, G. Chen, *Corros Sci*., 127 **(**2017) 70.
17. M. Yasri, B. Lescop, E. Diler, F. Gallée, D. Thierry, S. Rioual, *Sensors Actuat B-Chem*., 257 **(**2018) 988.
18. A. Prylepa, *J Phys D Appl Phys*., 51 **(**2018) 1.
19. R.N. Parkins, *Corros Sci*., 20 **(**1980) 147.
20. R.N. Parkins, R.N. Parkins (Ed.), Life Prediction of Corrodible Structures, vol. 1 NACE International, 1994, p. 97.
21. R.N. Parkins, A Review of Stress Corrosion Cracking of High Pressure Gas Pipelines, Corrosion/2000, Paper No. 00363.
22. B. Gu, J. Luo, X. Mao*, Corrosion*, 55 **(**1999) 96.
23. L.J. Qiao, J.L. Luo, X. Mao, *Corrosion*, 54 **(**1998) 115.
24. Y.F. Cheng, *Int J Hydrogen Energ*., 32 **(**2007) 1269.
25. F.F. Eliyan, E. Mahdi, A. Alfantazi, *Int J Electrochem Sci.,* 8 (2013) 578.
26. National Energy Board of Canada, Public inquiry concerning stress corrosion cracking on canadian

oil and gas pipelines, Report of the Inquiry, MH-2-95 (National Energy Board, Canada, 1996), p.11.
27. J. Castrellon-Uribe, M.E. Nicho, G. Reyes-Merino, *Sens Actuators B Chem*., 141 **(**2009) 40.
28. X. Liu, X. Mao, *Scripta Metall Mater*., 33 (1995) 145.
29. H.M. Ha, I.M. Gadala, A. Alfantazi, *Electrochim Acta*, 204 (2016) 18.
30. L. Rena, T. Jianga, Z. Jiab, D. Lia, C. Yuana, H. Lia, *Measurement,* 122 (2018) 57.